Supplementary Materials for

Pulmonary Neuroendocrine Cells Amplify Allergic Asthma Responses

Authors: Pengfei Sui[1,2], Darin L. Wiesner[3], Jinhao Xu[1,2], Yan Zhang[1,2], Jinwoo Lee[4], Steven Van Dyken[4], Amber lashua[2], Chuyue Yu[5], Bruce S. Klein[3], Richard M. Locksley[4], Gail Deutsch[6] and Xin Sun[1,2,*]

***Correspondence to:** xinsun@ucsd.edu.

This PDF file includes:

Figs. S1 to S25
Tables S1 to S3

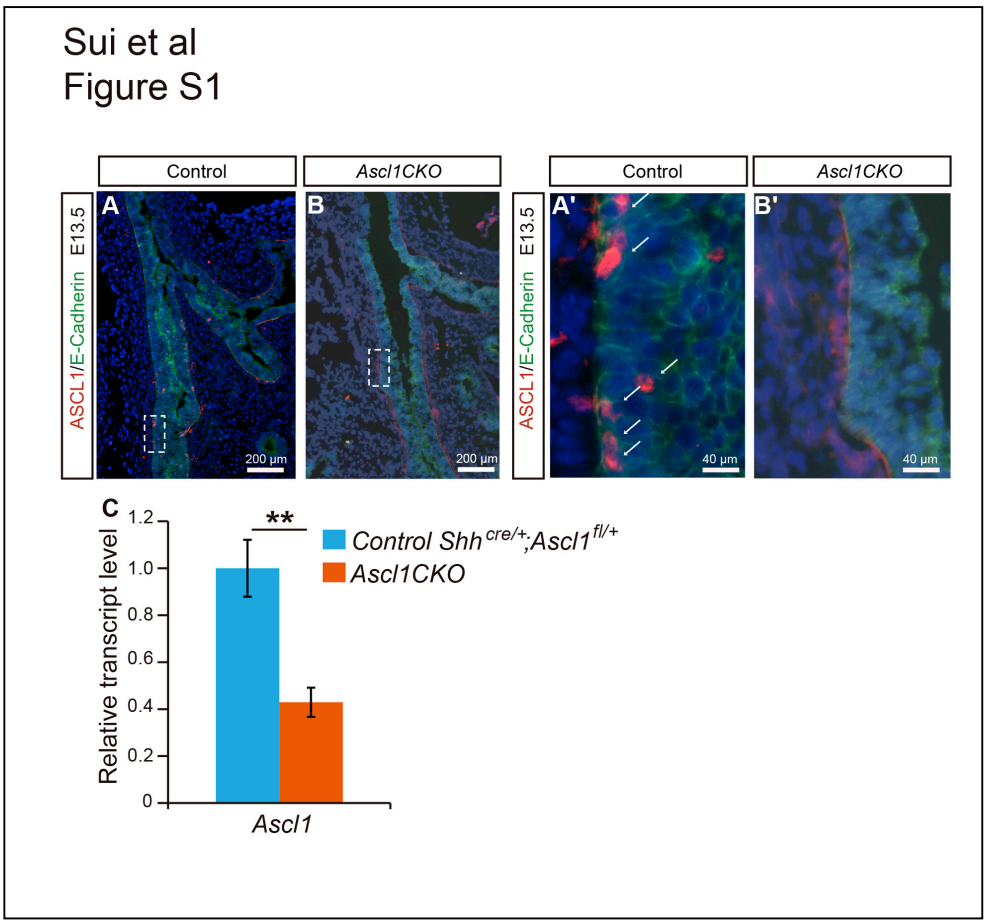

Fig. S1. Specific inactivation of *Ascl1* in the airway epithelium.

(A,B,A',B') At E13.5, ASCL1 and E-Cadherin double staining outlines ASCL1 expression in the epithelium. Boxed areas in A and B are magnified in A' and B', respectively. Arrows indicate ASCL1 signal in the epithelium in the control. No ASCL1 signal is detected in the *Ascl1CKO* epithelium, confirming inactivation. (C) qRT-PCR of *Ascl1* expression in E13.5 whole lungs. The controls are $Shh^{cre};Ascl1^{fl/+}$ heterozygous mutants. The residual expression in the mutant is likely due to expression in the intrinsic neurons which is not affected by Shh^{cre}. ** for $p < 0.01$. Student's *t*-test was used. Data are representative of three experiments. Error bars represent mean +/- SEM.

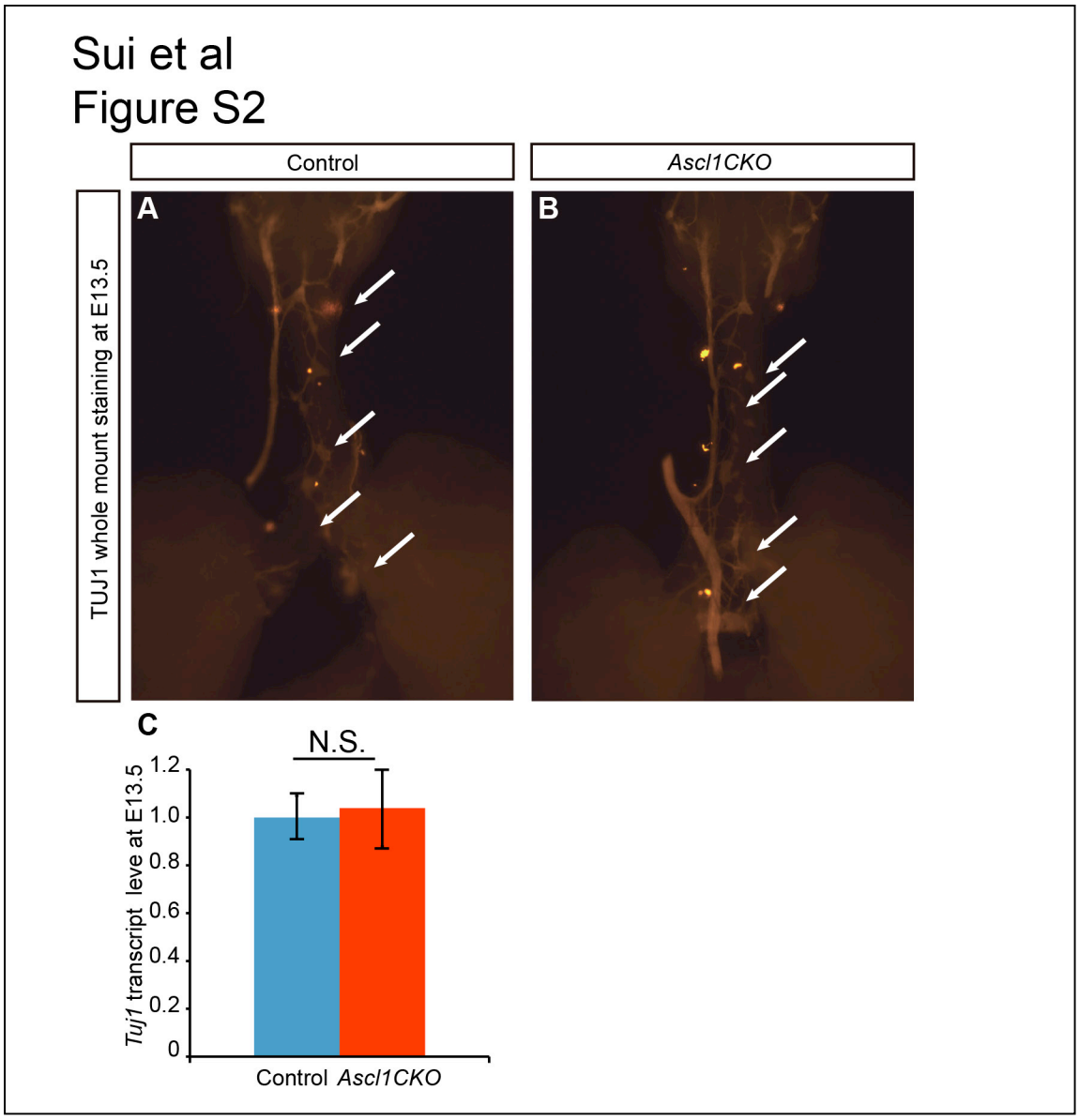

Fig. S2. Intrinsic neurons remain present in *Ascl1CKO* mutants.

(A) At E13.5, anti-TUJ1 staining indicated that intrinsic neurons (arrow) and associated nerves remain present in the *Ascl1CKO* mutant. (B) At E13.5, qRT-PCR analysis of *Tuj1* indicated similar expression level in *Ascl1CKO* lung compared to control. N.S. for not significant, $p \geq 0.05$. Student's *t*-test was used. Data are representative of three experiments. Error bars represent mean +/- SEM.

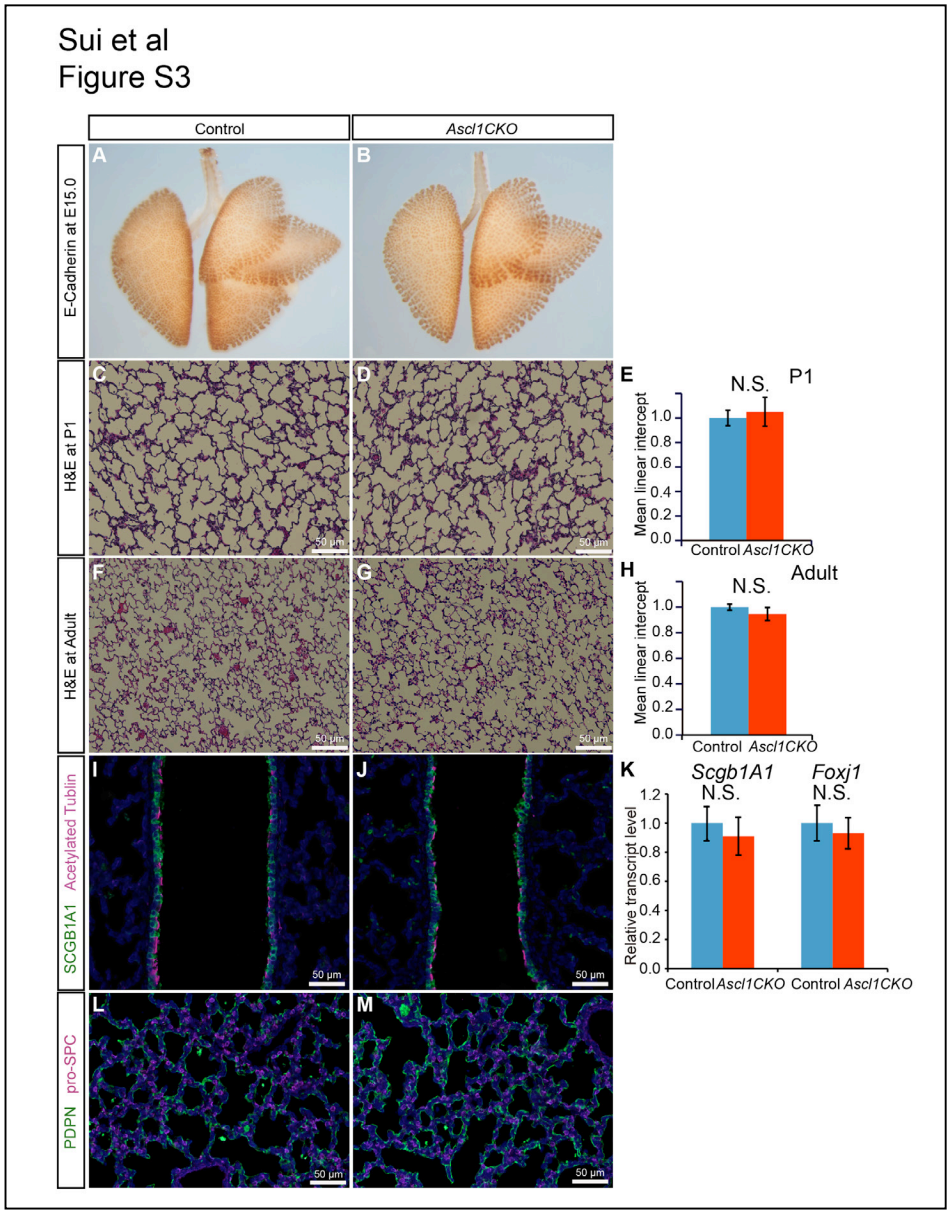

Fig. S3. Other aspects of lung development are normal in the *Ascl1CKO* mutant.

(A,B) Wholemount anti-E-cadherin staining indicated normal lung branching. (C-H) H&E staining showed normal alveolar morphology, as quantified by mean linear intercept analysis. (I,J) Anti-SCGB1A1 staining for club cells (green) and anti-acetylated tubulin staining for ciliated cells (magenta) showed normal airway epithelial cell differentiation. (K) qRT-PCR of *Scgb1a1* and *Foxj1* expression in control and *Ascl1CKO* mice at P1. (L,M) Anti-PDPN staining for AT1 cells (green) and anti-pro-SPC staining for AT2 cells (magenta) showed normal alveolar epithelial cell differentiation. n = 3 for each group. N.S. for not significant, $p \geq 0.05$. Student's *t*-test was used. Data are representative of three experiments. Error bars represent mean +/- SEM.

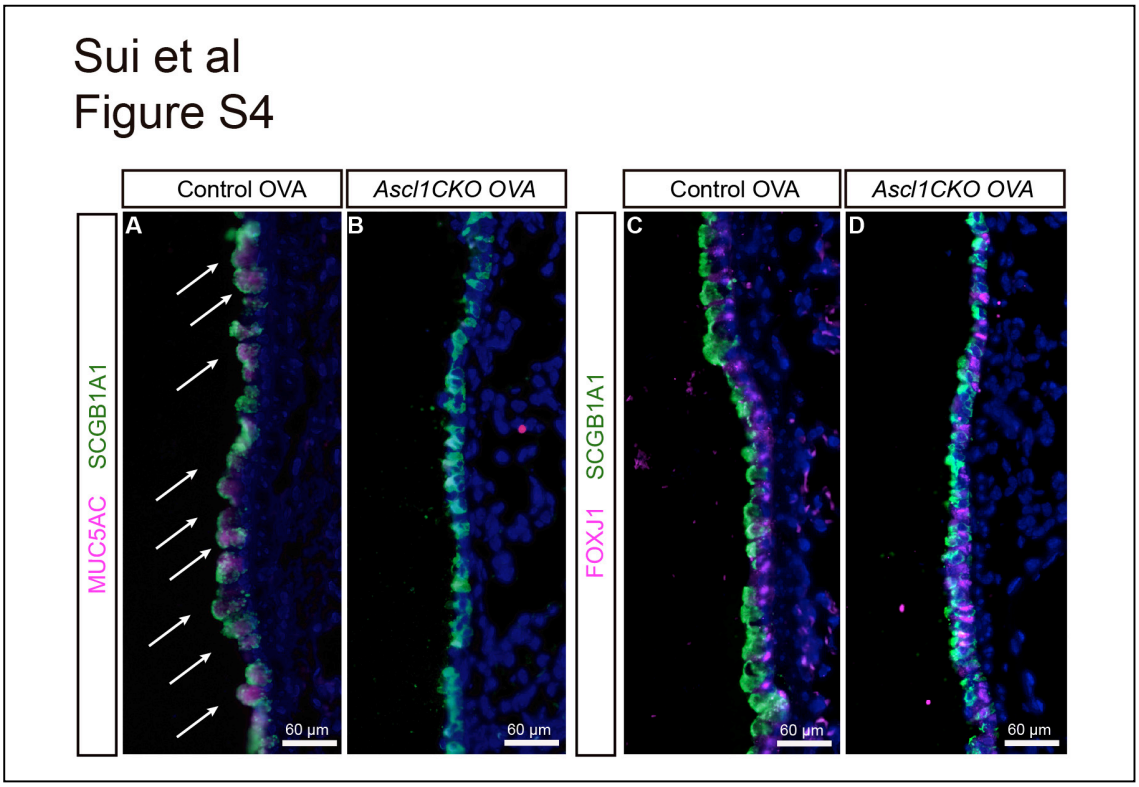

Fig. S4. Airway epithelial cell marker expression in OVA-challenged heterozygous control and *Ascl1CKO* mice.

(A,B) Representative anti-MUC5AC staining for goblet cells (magenta) and anti-SCGB1A1 staining for club cells (green) showed overlap of goblet and club cell markers in the control airway, but no MUC5AC staining in *Ascl1CKO* airway. (C,D) Representative anti-SCGB1A1 (green) and anti-FOXJ1 (magenta) co-staining showed normal club and ciliated cell proportion in *Ascl1CKO* mice even after OVA challenge. Data are representative of three experiments.

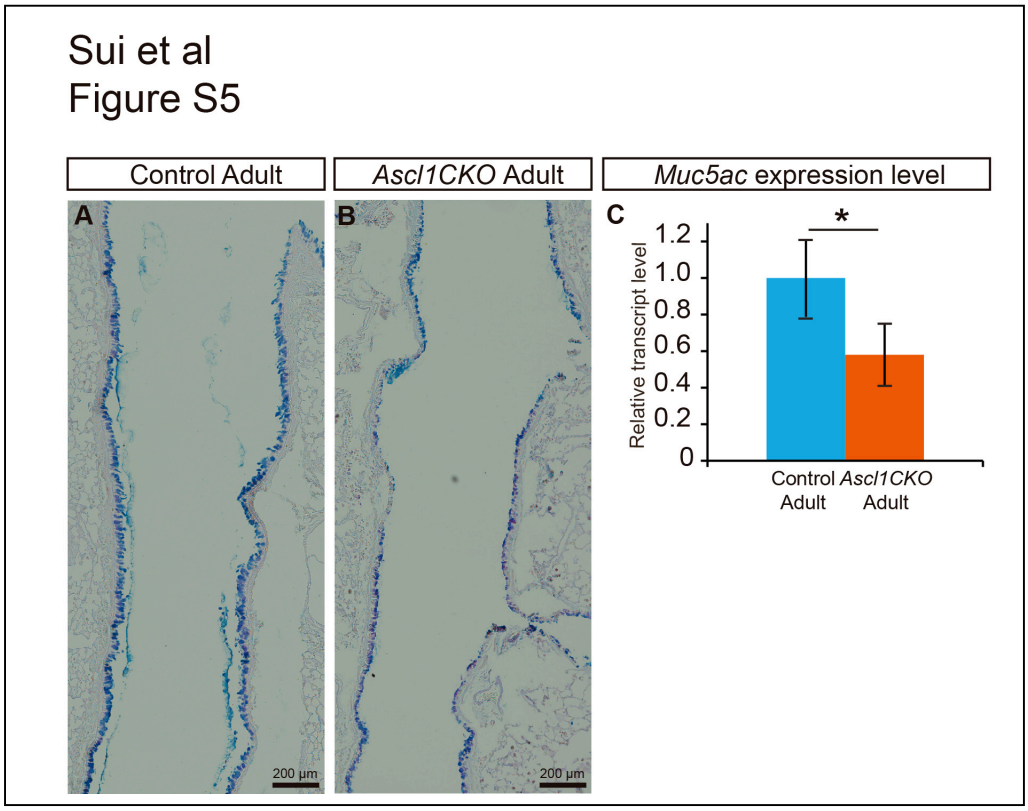

Fig. S5. PNECs play a role in goblet cell hyperplasia in adult HDM asthma model.

(A,B) Representative PAS staining of adult longitudinal airway sections of HDM challenged control and *Ascl1CKO* mice. (C) qRT-PCR of *Muc5ac* expression in HDM challenged control and *Ascl1CKO* lungs. n = 3 for each group. * for $p < 0.05$. Student's *t*-test was used. Data are representative of three experiments. Error bars represent mean +/- SEM.

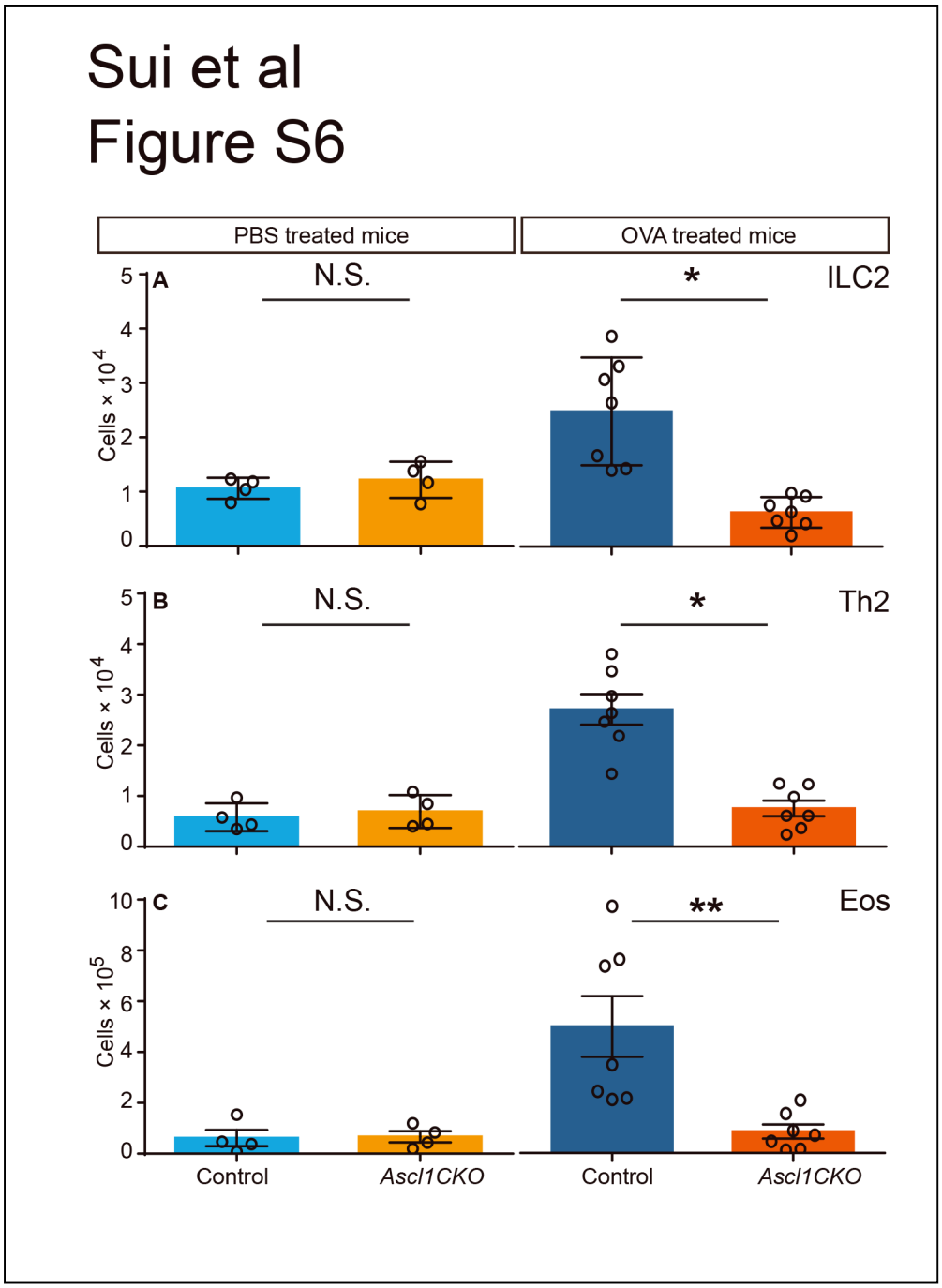

Fig. S6. PNECs are required for type 2 immune response following OVA challenge.

(A-C) Total cell numbers from flow cytometric analysis of immune cells from whole lungs, after either OVA or control PBS challenge as labeled. Student's *t*-test was used. n = 4 for PBS groups, and n = 7 for OVA groups. N.S. for not significant $p \geq 0.05$, * for $p < 0.05$, ** for $p < 0.01$. Student's *t*-test was used. Data are representative of three experiments. Error bars represent mean +/- SEM.

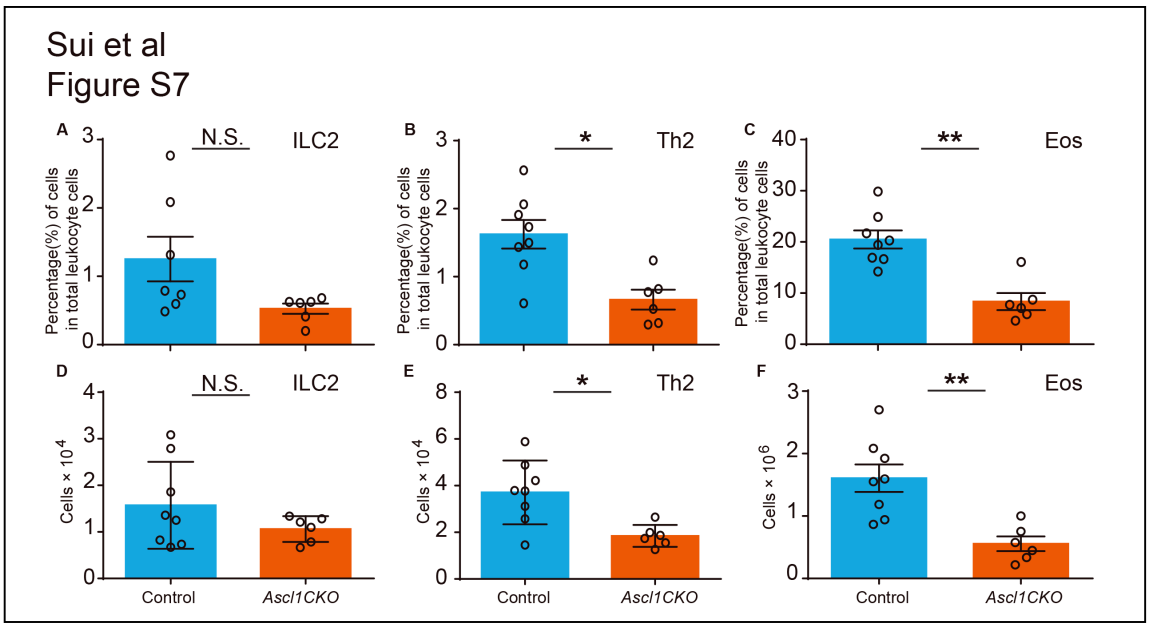

Fig. S7. PNECs are required for T_h2 response in adult HDM asthma model.

(A-F) Flow cytometric analysis of immune cells from HDM challenged control or *Ascl1CKO* mutant adult lungs. Data are representative of three experiments. Mann/Whitney *U* test was used. n = 8 for controls, n = 6 for mutants. N.S. for not significant $p \geq 0.05$, * for $p < 0.05$, ** for $p < 0.01$. Error bars represent mean +/- SEM.

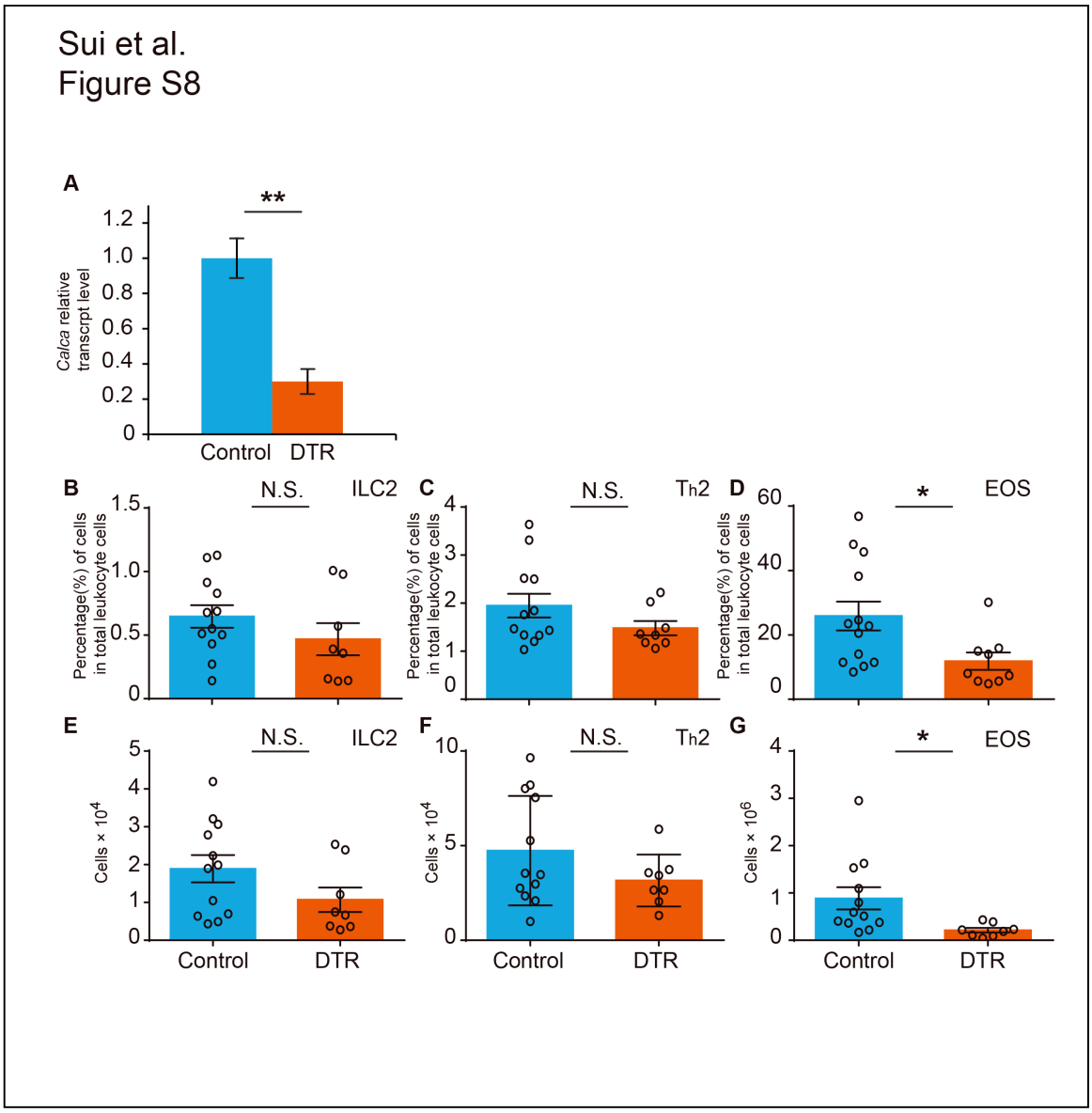

Fig. S8. Postnatal ablation of PNECs dampened HDM induced T_h2 response.

(A) qRT-PCR of *Calca* (encoding CGRP) expression in the lungs from DTX treated control or DTR (*Shh*^{cre}*;Calca-lox-GFP-lox-DTR*)-expressing mice, indicating the extent of ablation. Student's *t*-test was used. n=3 for each group. (B-G) Flow cytometric analysis of indicated immune cells from DTX treated then HDM treated control and DTR-expressing mice. Data are presented as cell % (B-D) or total cell number (E-G). Data are representative of three experiments. Mann/Whitney *U* test was used. n = 8 for control, n = 6 for mutants. N.S. for not significant $p \geq 0.05$, * for $p < 0.05$, ** for $p < 0.01$. Error bars represent mean +/- SEM.

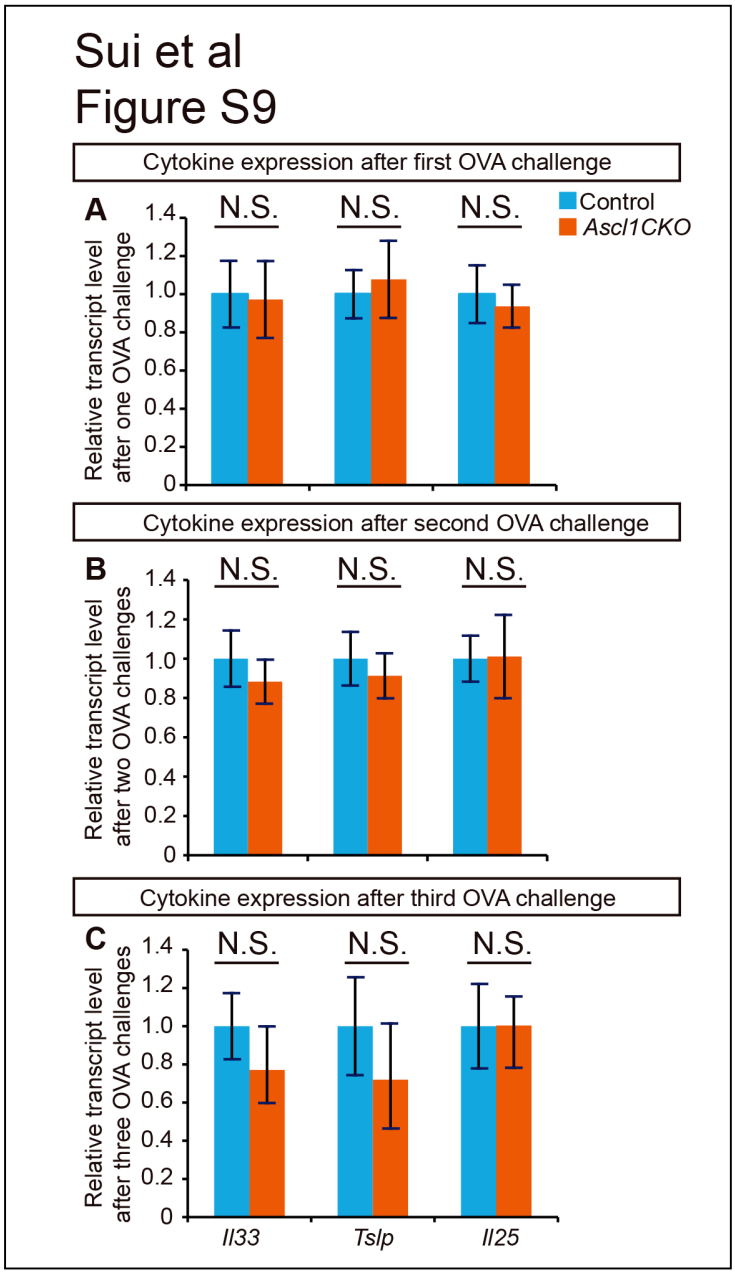

Fig. S9. Epithelium-derived cytokine expression is similar in the *Ascl1CKO* mutant compared to control after OVA challenge.

(A-C) qRT-PCR analysis of cytokine expression in whole lung after one, two or three neonatal OVA challenges. Data are representative of three experiments. Student's *t*-test and standard error of the mean were used. n = 3 for each group. N.S., not significant, $p \geq 0.05$. Error bars represent mean +/- SEM.

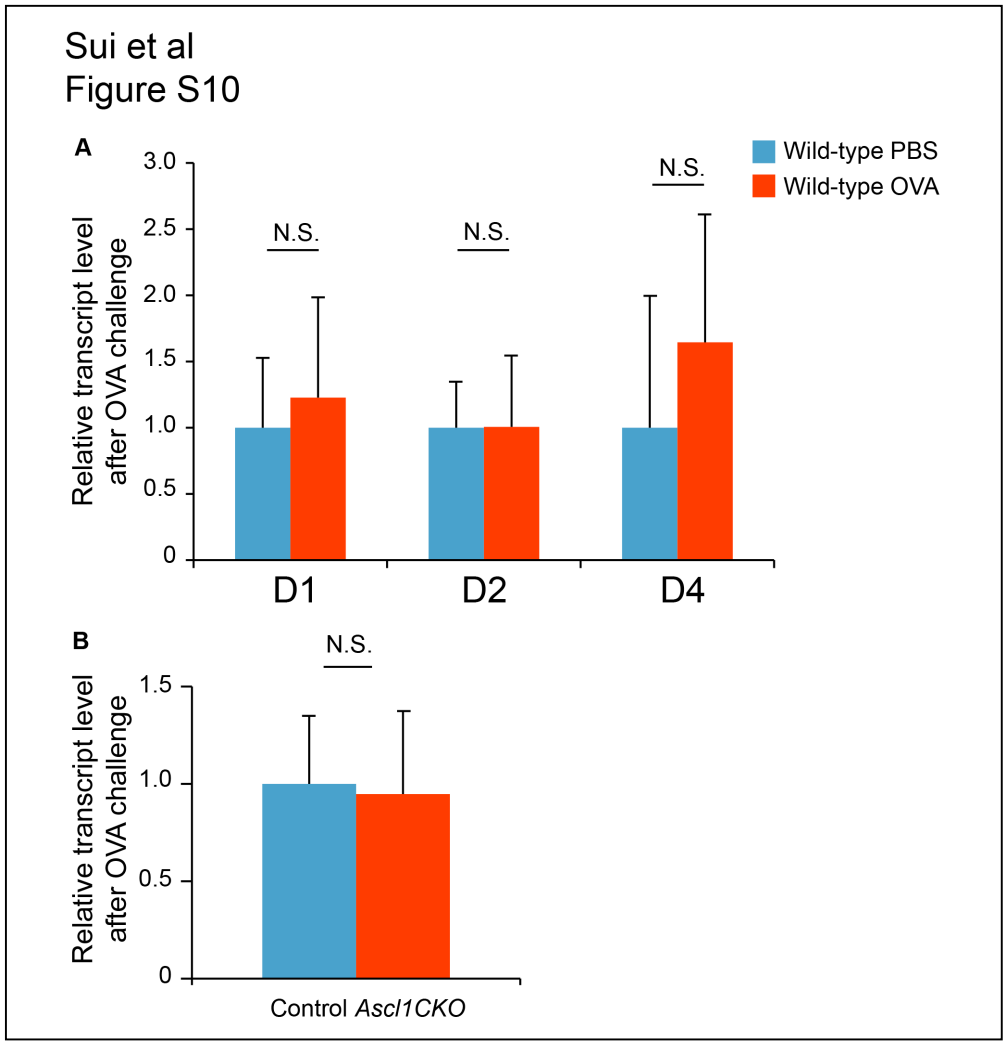

Fig. S10. Neuronal *Calca* expression is not altered during allergic asthma response.

(A) qRT-PCR of vagal ganglia *Calca* expression in neonatal OVA treated compared to PBS treated C57Bl/6 wild-type mice at D1, 2, and 4 (P21, 22, and 24 respectively) after the start of OVA challenge. Through multiple experiments, large variations are consistently observed in both PBS and OVA group as a feature of the variable *Calca* expression in vagal ganglia neurons. (B) qRT-PCR of vagal ganglia *Calca* expression in OVA treated control and *Ascl1CKO* mice at D4 after the start of OVA challenge (P24). Student's *t*-test was used. n = 3 for each group, and each sample contained vagal ganglion from at least two mice. N.S., not significant, $p \geq 0.05$. Error bars represent mean +/- SEM. Data are representative of three experiments.

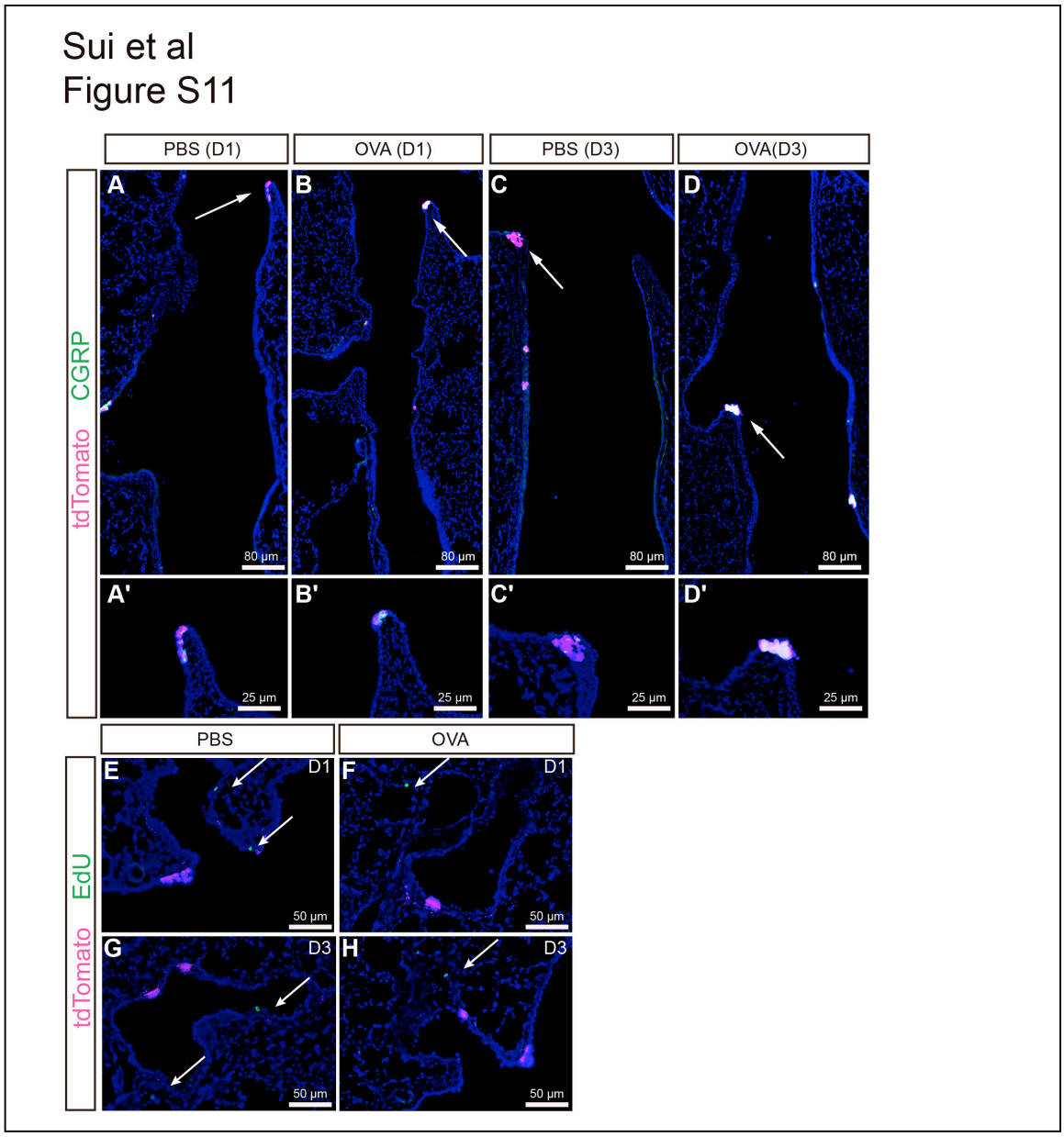

Fig. S11. CGRP is increased in intensity and remains restricted to PNECs in airway epithelium during allergic asthma response.

(A-D,A'-D') Representative images of *Ascl1*^{creERT2}*;tdTomato* lineage labeling of PNECs and anti-CGRP staining at either D1 or D3 after the start of neonatal OVA challenge. Arrows point to clusters of PNECs that are magnified in lower panels. Overlap of signals indicates that in the airway epithelium, CGRP remains restricted to PNECs after OVA challenge. Compared to PBS, in the OVA-treated lungs, CGRP signal (green) is slightly increased at D1, and clearly increased at D3 of challenge. (E-H) Representative images of EdU staining (green, arrows) in lung. In both the PBS and neonatal OVA-treated lungs at either D1 or D3 of challenge, there was no EdU-positive, tdTomato-lineage PNECs. n = 4 for each group. Data are representative of two experiments.

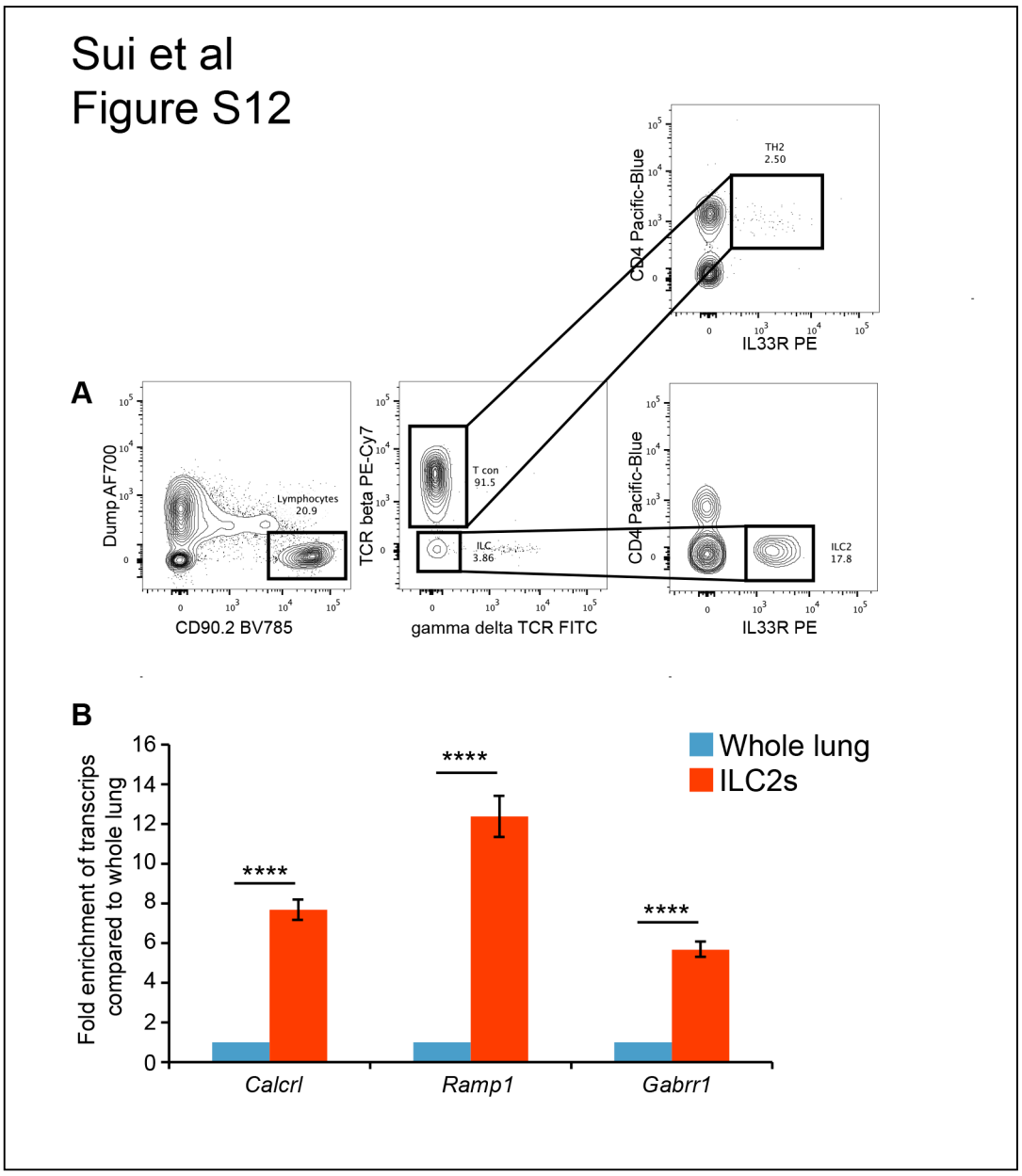

Fig. S12. CGRP and GABA receptor transcripts are enriched in ILC2s sorted from lung.

(A) Representative plots from sorting of ILC2s and T_h2 cells from wild-type naïve lungs. (B) qRT-PCR analysis of transcripts in sorted primary ILC2s from wild-type lung compared to whole lung for co-receptor genes for CGRP: *Calcrl* and *Ramp1*, and receptor gene for GABA: *Gabbr1*. ****p < 0.0001. Student's *t*-test was used. Data are representative of three experiments. Error bars represent mean +/- SEM.

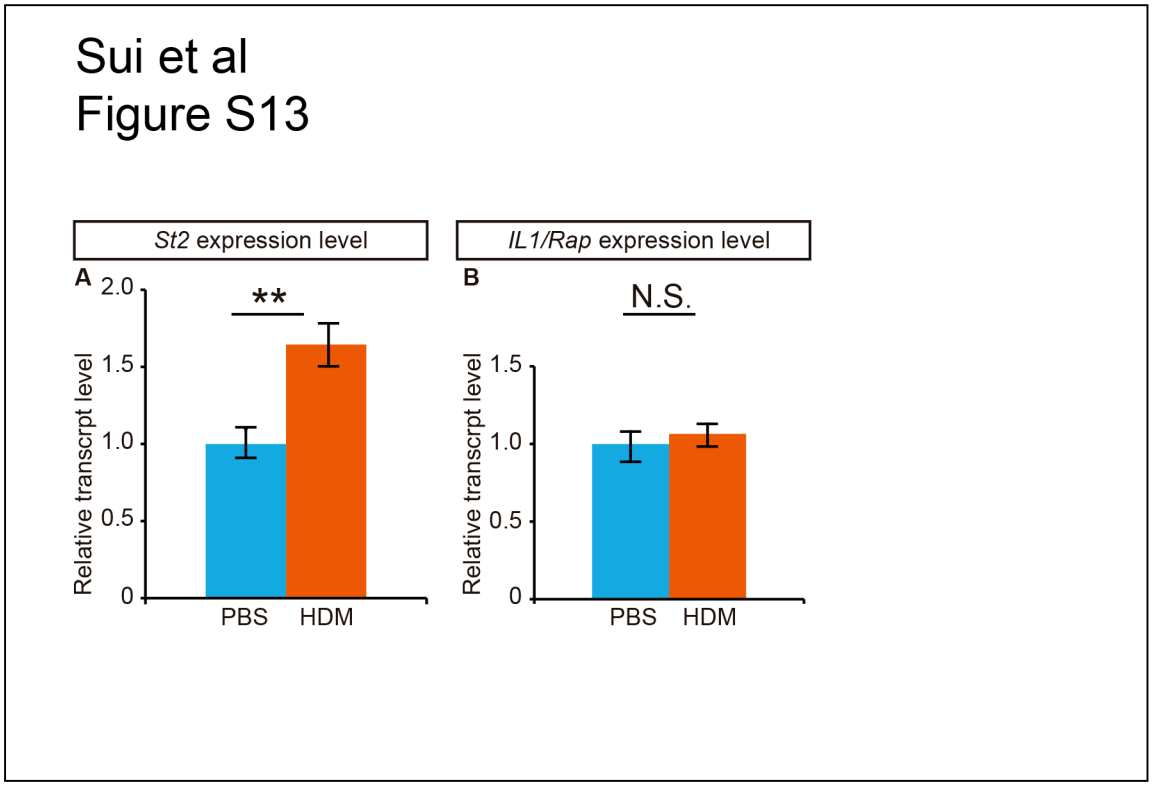

Fig. S13. Allergen challenge increased *St2* but not *IL1/Rap* transcript level in ILC2 cells.

(A,B) qRT-PCR of *St2* and *IL1/Rap* in primary ILC2 cells sorted from lungs of PBS or HDM treated adult mice. Data are representative of two experiments. Student's *t*-test was used. n = 3 for each group. N.S. for not significant, $p \geq 0.05$, ** for $p < 0.01$. Error bars represent mean +/- SEM.

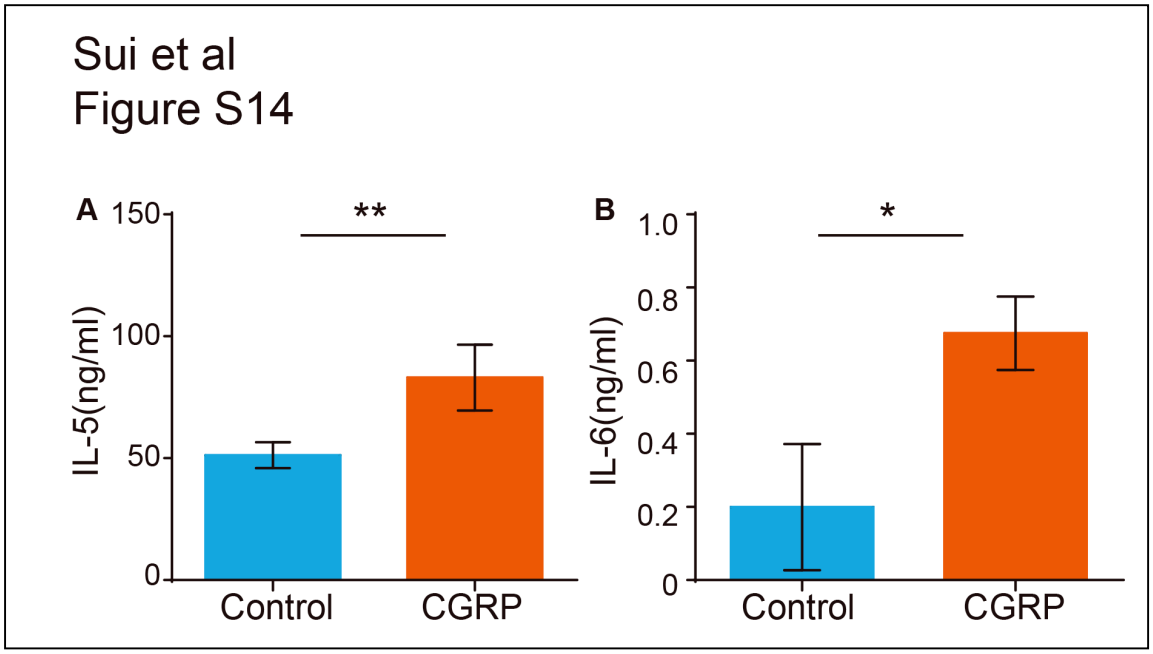

Fig. S14. CGRP peptide increased IL-5 and IL-6 production from ILC2 cells.

(A,B) IL-5 or IL-6 production by sorted ILC2 cells in culture in the presence of IL-7 and IL-33, with or without CGRP. IL-5 or IL-6 levels were measured using the LEGENDplex system. Data are representative of two experiments. Student's *t*-test was used. n = 3 for each group, * for $p < 0.05$, ** for $p < 0.01$. Error bars represent mean +/- SEM.

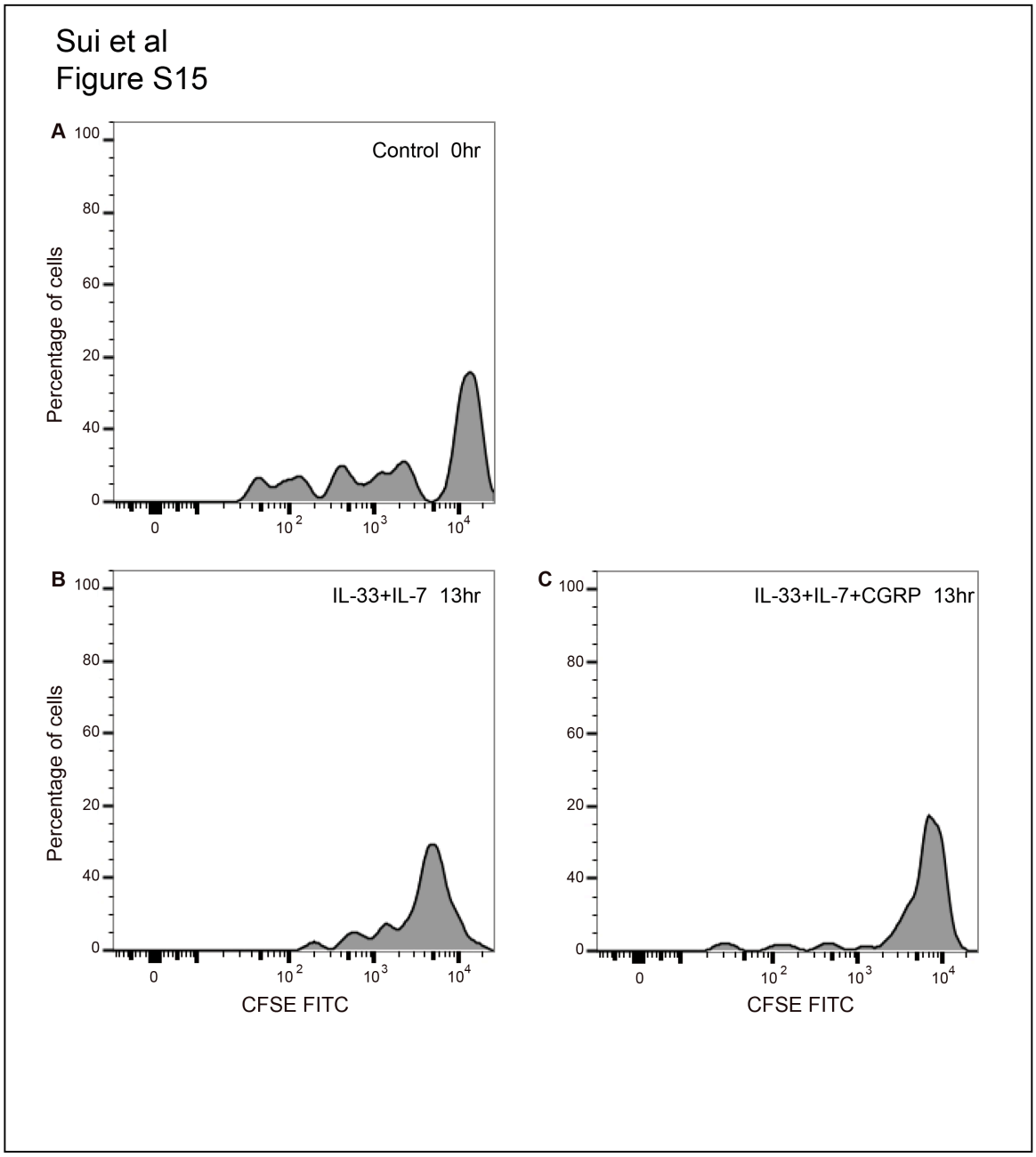

Fig. S15. CGRP does not change ILC2 number in culture.

(A-C) Analysis of CFSE stained ILC2s at the beginning of culture (A), or after 13 hours in culture with either IL-33+IL-7 (B), or IL-33+IL-7+CGRP (10 ng/ml for each of IL-33 and IL-7, 100 nM for CGRP) (C). Culturing with CGRP did not shift the peaks of CFSE-stained cells. Data are representative of two experiments.

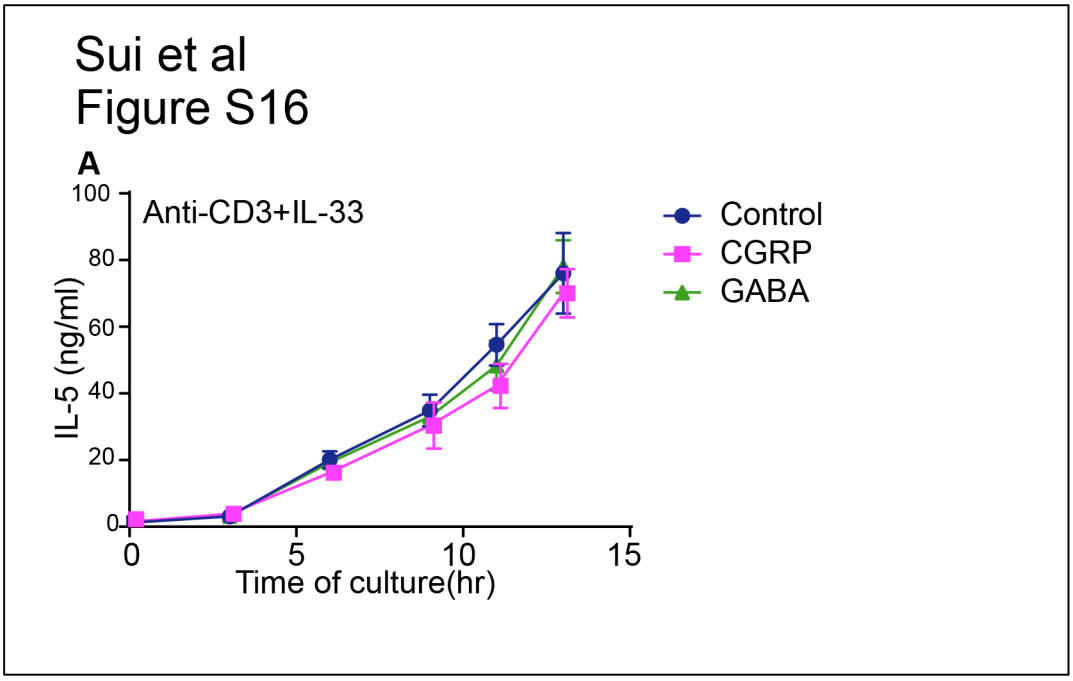

Fig. S16. T_h2 cells do not change their IL-5 production in response to CGRP or GABA.

Sorted primary T_h2 cells were cultured for up to 13 hours with anti-CD3 and IL-33 (10 ng/ml for each), and either CGRP (100 nM) or GABA (10 mM). Neither CGRP nor GABA led to a change in IL-5 secretion. Data are representative of two experiments. Student's *t*-test was used. n = 3 for each group, $p \geq 0.05$ at all-time points. Error bars represent mean +/- SEM.

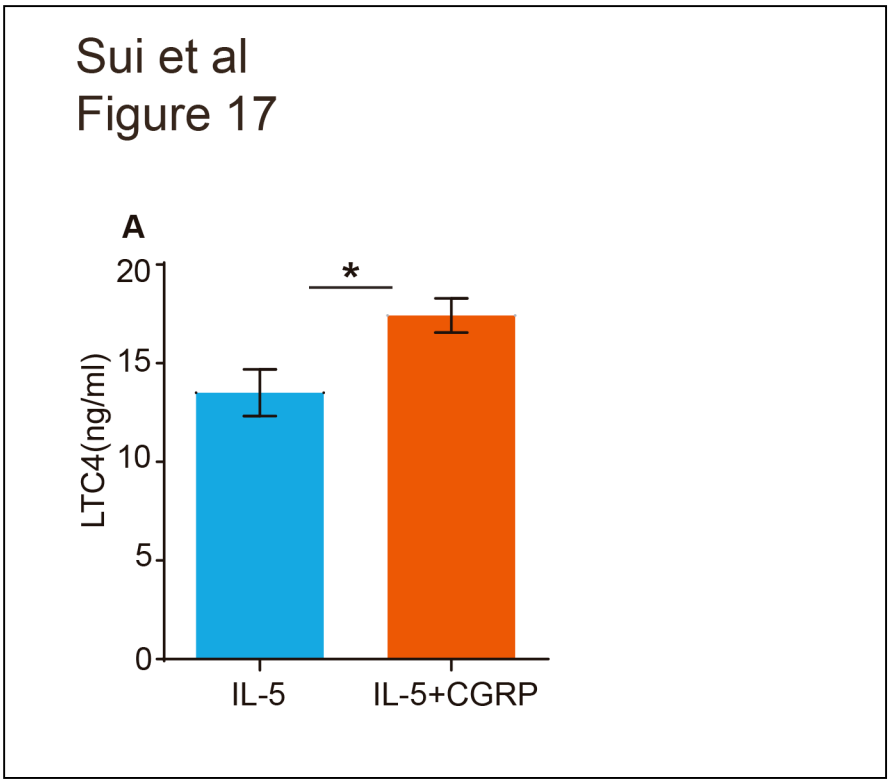

Fig. S17. CGRP effect on primary eosinophils.

(A) Sorted primary eosinophils were cultured in the presence of IL-5 with or without CGRP for 12 hours. Secreted Leukotriene C4 was measured using LTC4 ELISA kit. CGRP can slightly increase LTC4 production in vitro. Data are representative of two experiments. Student's *t*-test was used. n = 3 for each group, * for $p < 0.05$.

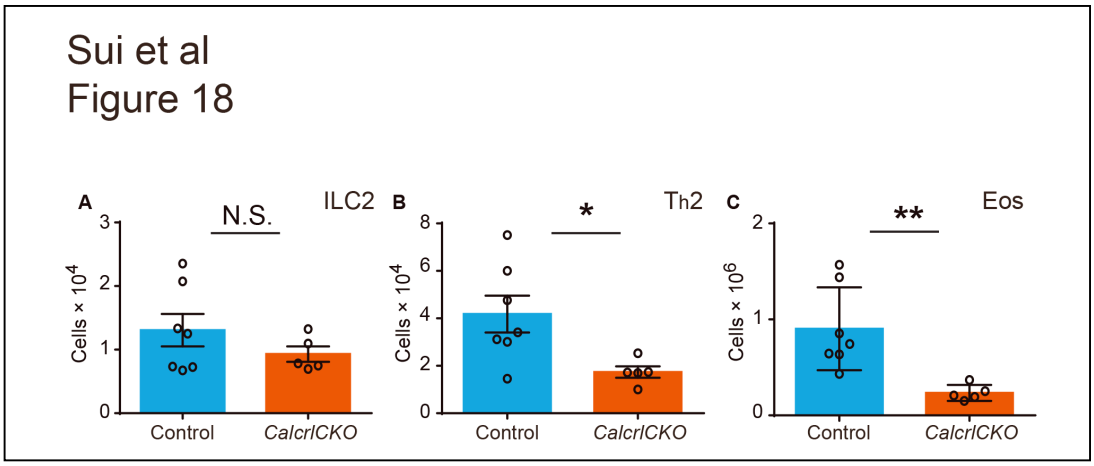

Fig. S18. Type 2 immune cell numbers are reduced in *CalcrlCKO* mutant compared to control after HDM challenge.

Flow cytometric analysis of immune cell number in whole lungs after HDM challenge. Mann/Whitney *U* test was used. n = 7 for controls, n = 5 for mutants. N.S. for not significant, $p \geq 0.05$, * for $p < 0.05$, ** for $p < 0.01$. Data are representative of three experiments. Error bars represent mean +/- SEM.

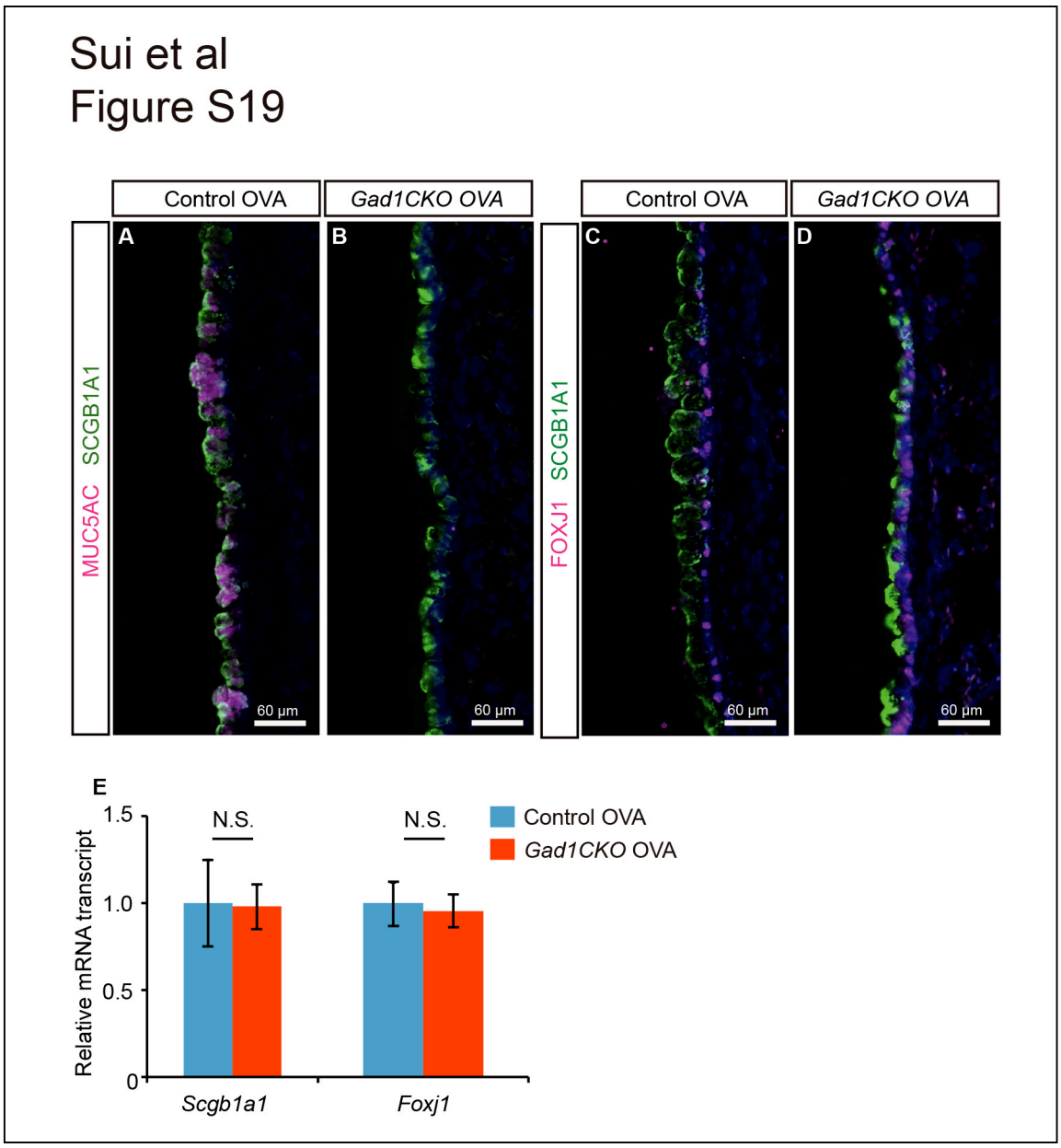

Fig. S19. Airway epithelial cell marker expression in the *Shh*^{cre};*Gad1*$^{fl/fl}$ mutant.

(A,B) Representative anti-MUC5AC staining for goblet cells (magenta) and anti-SCGB1A1 staining for club cells (green) showed presence of MUC5AC signal in the club cells in the control, and lack of MUC5AC signal in the mutant after OVA. (C,D) Representative anti-SCGB1A1 (green) and anti-FOXJ1 (red) co-staining showed normal club and ciliated cell proportion in *Gad1CKO* lungs after OVA. Data are representative of sections from three mice. (E) qRT-PCR of *Scgb1a1* and *Foxj1* expression in control and *Gad1CKO* lungs after OVA. Data are representative of three experiments. Student's *t*-test was used. n = 3 for each group. N.S. for not significant, $p \geq 0.05$. Error bars represent mean +/- SEM.

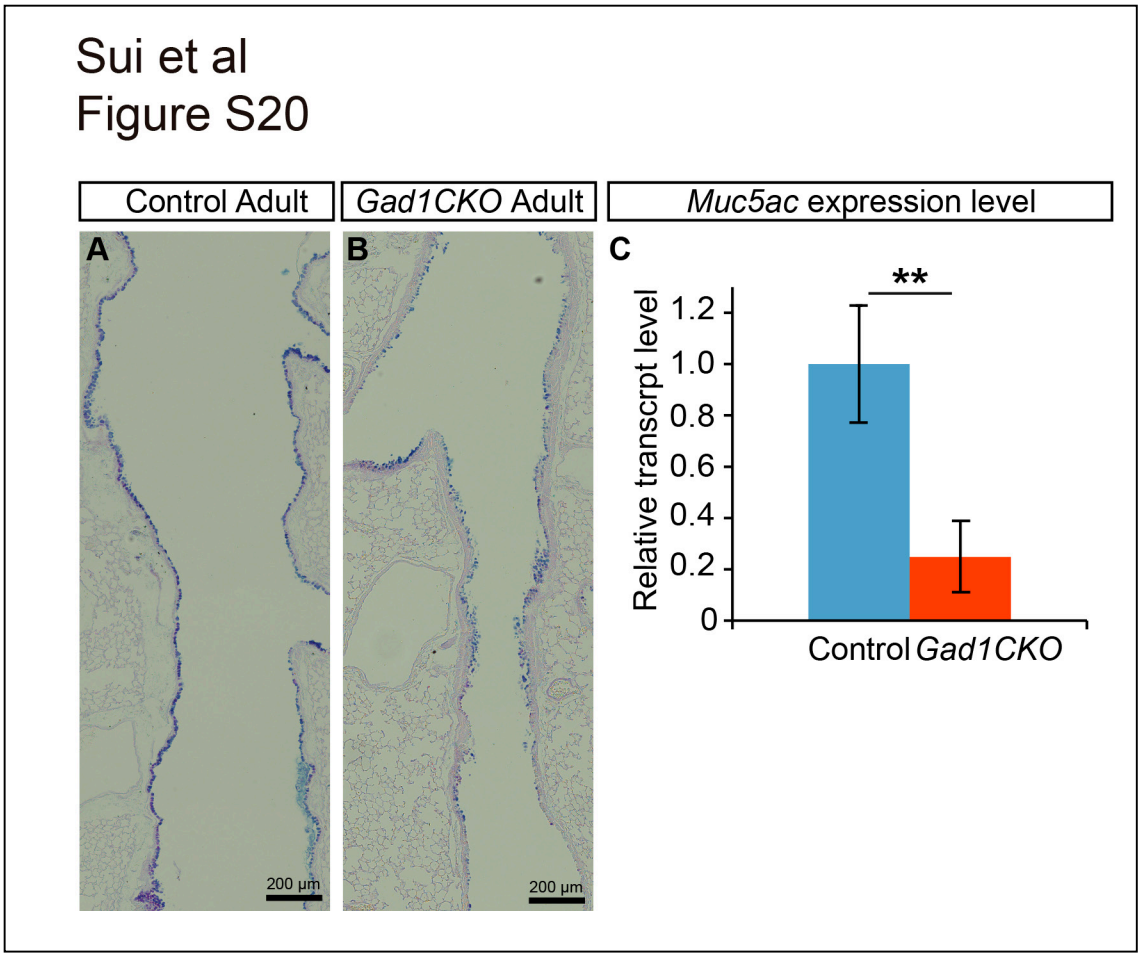

Fig. S20. *Gad1* is required for goblet cells hyperplasia following allergen challenge in the adult.

(A,B) Representative PAS staining of adult longitudinal airway sections of OVA challenged control and *GAD1CKO* mice. (C) qRT-PCR of *Muc5ac* expression in OVA challenged control and *Gad1CKO* lungs. Data are representative of three experiments. Student's *t*-test was used. n = 3 for each group. ** for $p < 0.01$. Error bars represent mean +/- SEM.

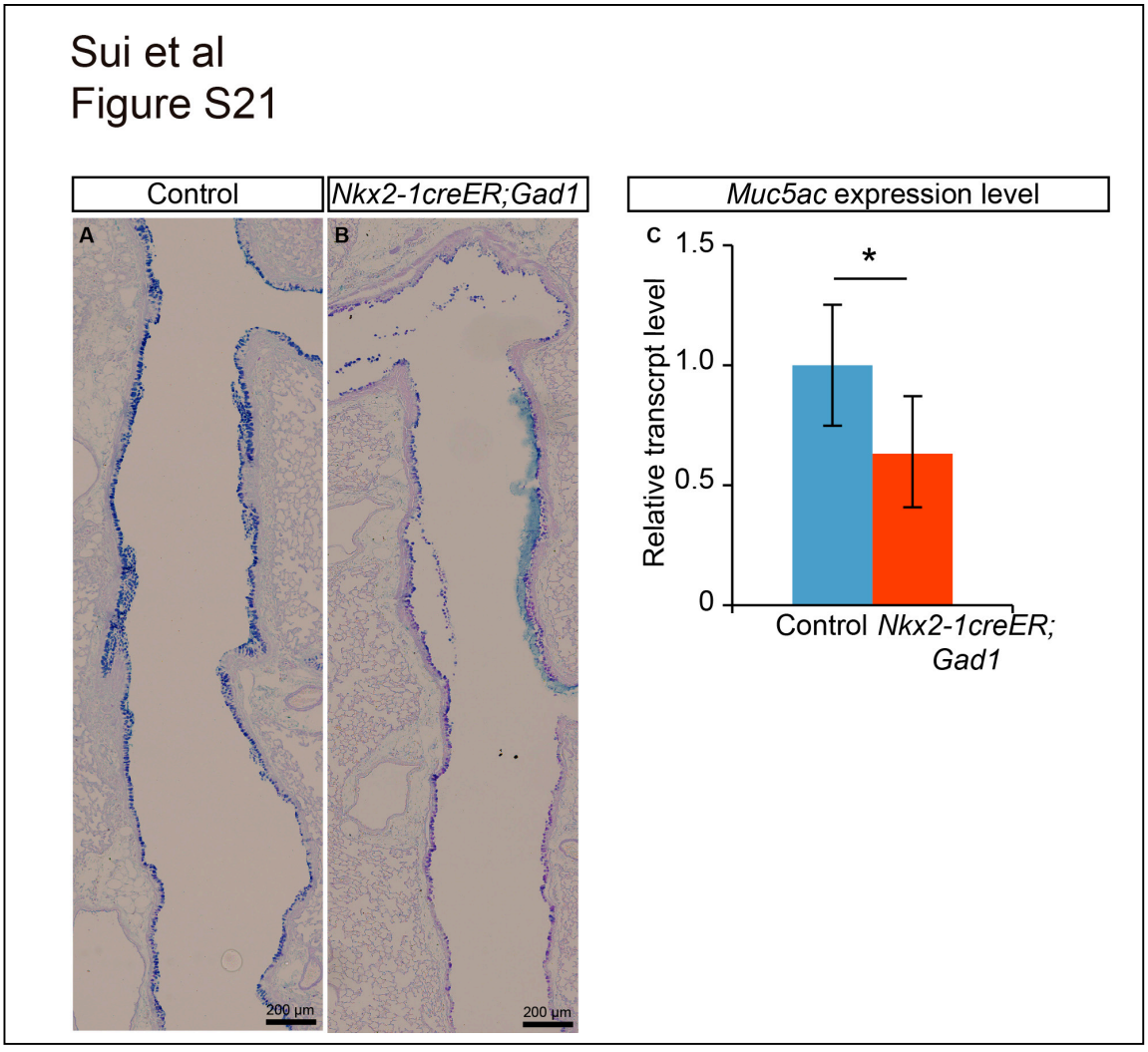

Fig. S21. *Nkx2-1*^{creERT2}*;Gad1*$^{fl/fl}$ mutant mice showed reduced goblet cell hyperplasia following allergen challenge.

(A,B) Representative PAS staining of adult longitudinal airway sections of OVA challenged control and *Nkx2.1*^{creERT2}*;Gad1*$^{fl/fl}$ (thereafter *Nkx2-1*^{creER}*;Gad1*) mice. (C) qRT-PCR of *Muc5ac* expression in HDM challenged control or *Nkx2-1*^{creER}*;Gad1* lungs. Data are representative of three experiments. Student's *t*-test was used. n = 3 for each group. * for $p < 0.05$. Error bars represent mean +/- SEM.

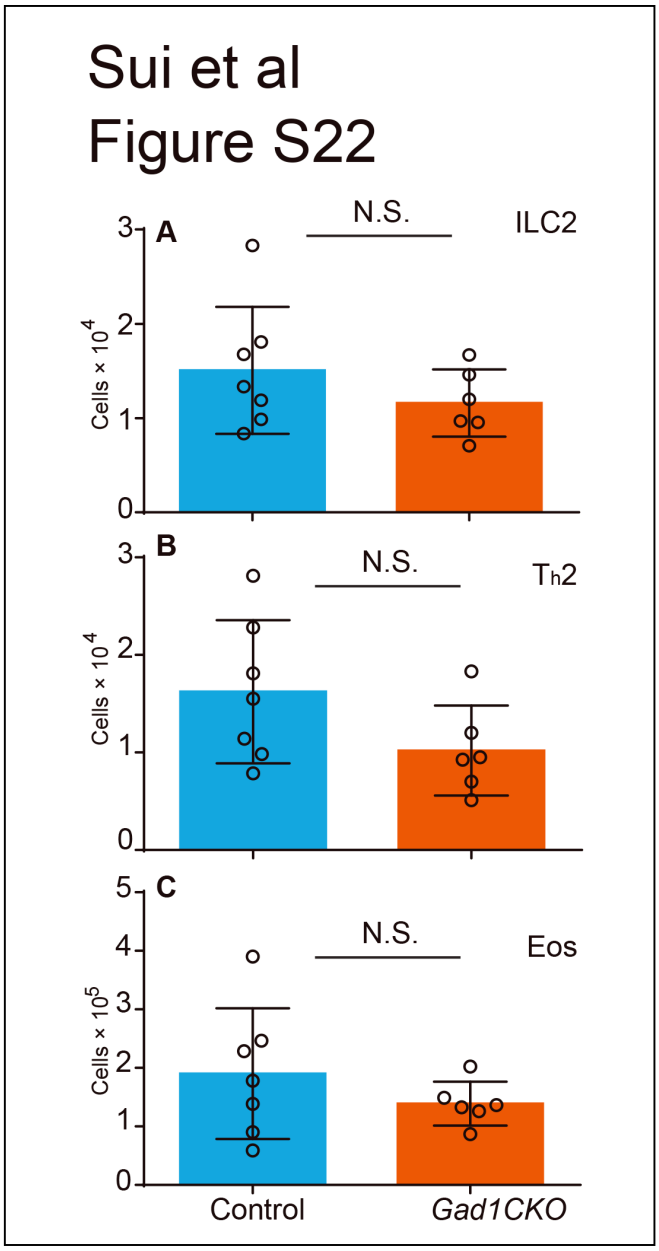

Fig. S22. Type 2 immune cell numbers are similar in the *Gad1CKO* mutant compared to control after OVA challenge.

Flow cytometric results of immune cell number in whole lungs after OVA challenge. n = 7 for controls and n = 6 for mutants. Data are representative of three experiments. Student's *t*-test was used. N.S. for not significant, $p \geq 0.05$. Error bars represent mean +/- SEM.

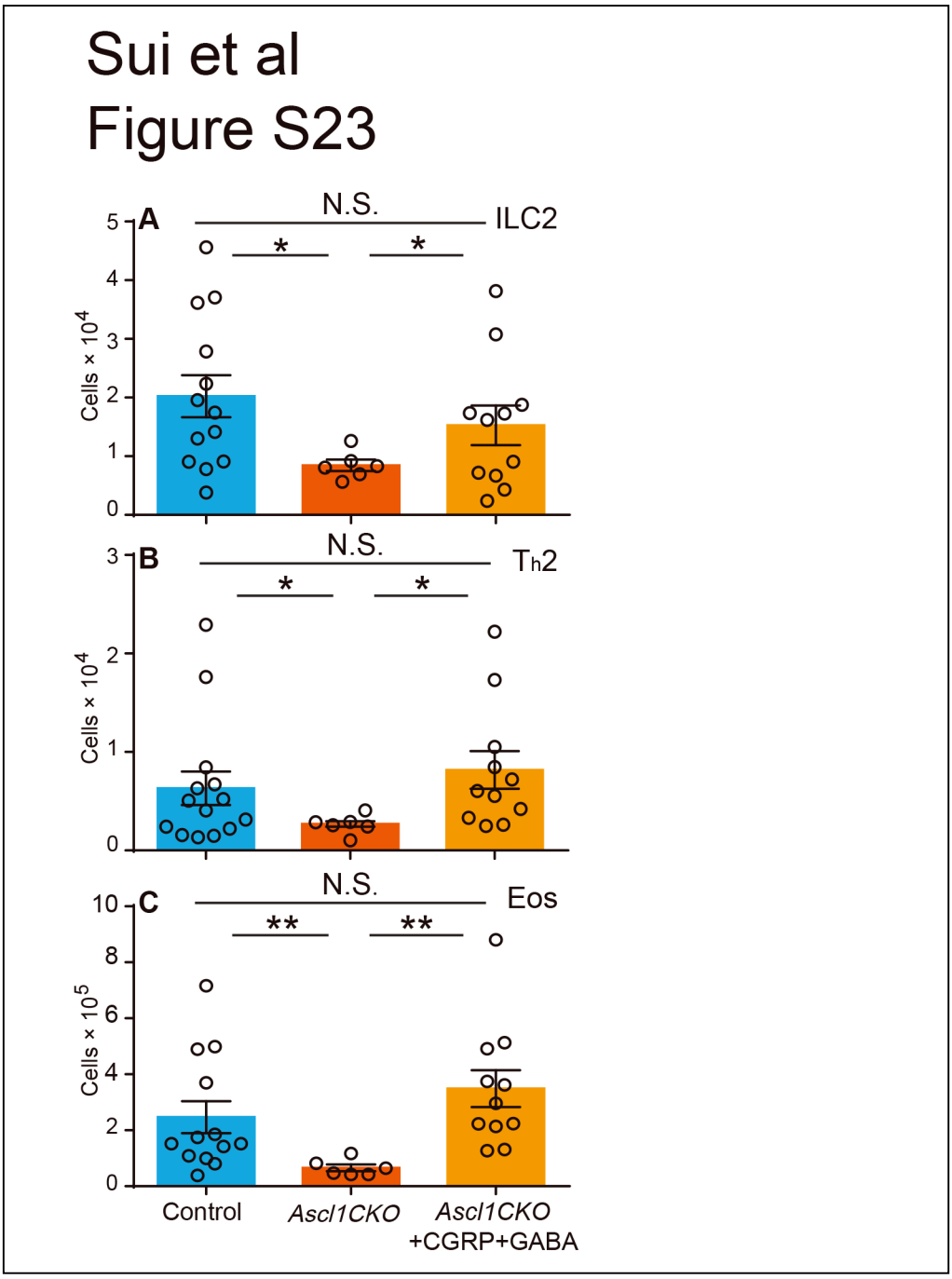

Fig. S23. Type 2 immune cell numbers are rescued in *Ascl1CKO* lungs with intra-tracheal instillation of CGRP and GABA.

Flow cytometric results of immune cell number in whole lungs after OVA challenge. n = 13 for control, n = 6 for *Ascl1CKO*, and n = 11 for *Ascl1CKO*+CGRP+GABA group. Student's *t*-test was used. N.S., not significant, $p \geq 0.05$, * for $p < 0.05$, ** for $p < 0.01$. Data are representative of three experiments. Error bars represent mean +/- SEM.

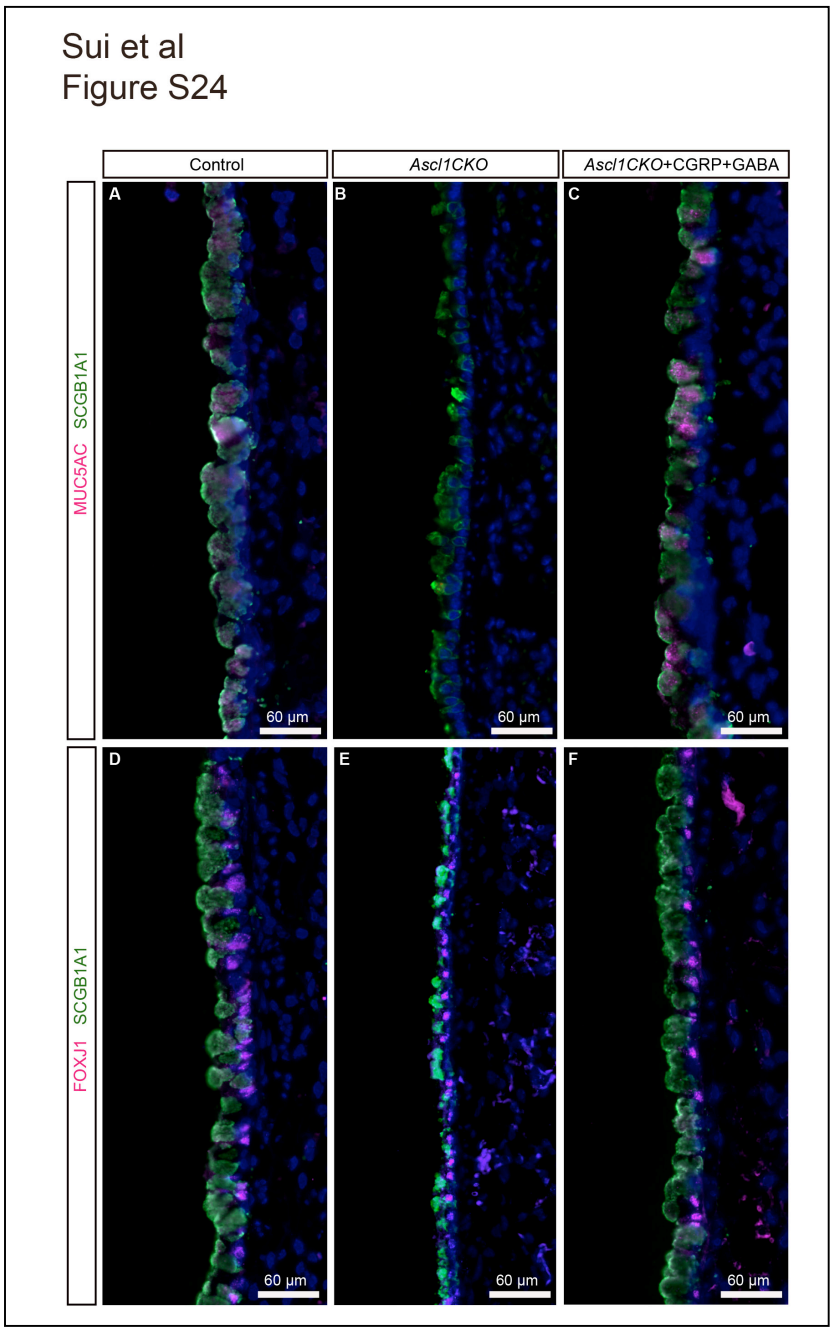

Fig. S24. Airway epithelial cell marker expression in lungs with intra-tracheal instillation of CGRP and GABA.

(A-C) Representative anti-MUC5AC staining for goblet cells (magenta) and anti-SCGB1A1 staining for club cells (green) showed that in *Ascl1CKO* mutant treated with CGRP and GABA, club cells express goblet cell marker, similar to control. (D-F) Representative anti-SCGB1A1 (green) and anti-FOXJ1 (magenta) co-staining showed normal proportion of club and ciliated cells in all groups. Data are representative of sections from three mice for each group.

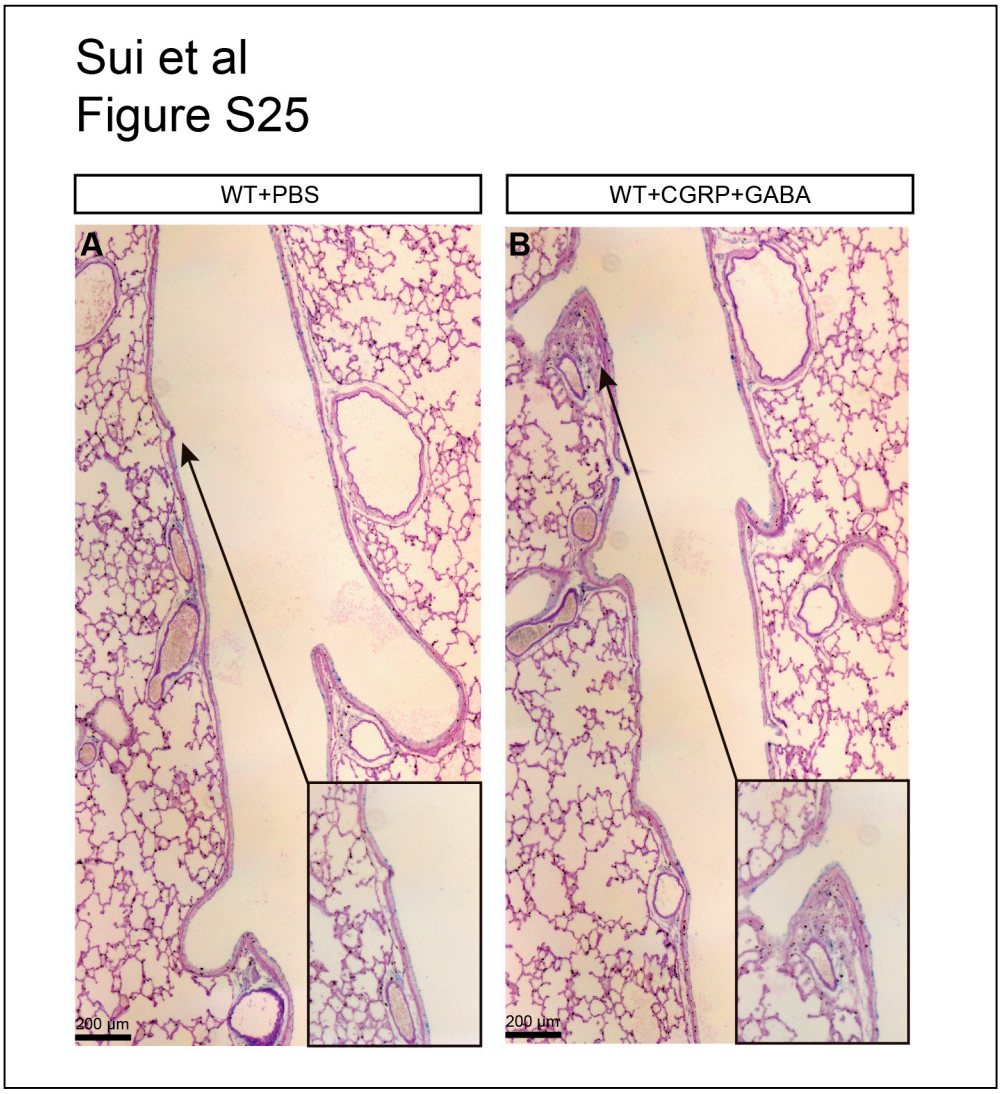

Fig. S25. CGRP and GABA instillation does not lead to baseline goblet cell hyperplasia in mice sensitized by OVA injection, but not challenged by OVA aerosol.

(A,B) PAS staining of P24 wild-type mouse airways. Arrows from insets point to areas that are magnified. (A) Mice sensitized with OVA i.p. injection, followed by intratracheal administration of PBS. (B) Mice sensitized with OVA i.p. injection, followed by intratracheal administration of CGRP and GABA. Without aerosolized OVA challenge, no PAS staining is observed in either group. Data are representative of sections from three mice for each group.

Table S1. RNAseq reads indicate that CGRP receptor gene expression is not significantly altered in *the Il33;Il25;Tslp* triple mutant ILCs.

	Calcrl		*Ramp1*	
	WT	Il33, IL25 and TSLP TKO	WT	IL33, IL25 and TSLP TKO
#1	2224	5797.5	4037.5	2348.1
#2	7568.1	5580.3	2037.4	2011.8
#3	11724.3	4266	1895.3	1903.2
#4	6752.6	7820.8	1828.9	2941.2
#5	9842.6		1483.4	
Average	7622.32(±3593.64)	5866.15(±1468.28)	2256.5(±1016.238)	2301.075(±466.88)

Table S2. Patient characteristics, treatment regime and primary autopsy findings.

Table S1	Age (year) at demise	Gender	History of lung disease	Other conditions	Medications	Cause of Demise
Asthma 1	9.2	Male	Asthma	None	Albuterol Steroid inhaler Antihistamine	Asthma exacerbation
Asthma 2	7.6	Female	Asthma	None	Albuterol Steroid inhaler Antihistamine	Asthma exacerbation
Asthma 3	11.4	Male	Asthma	None	Albuterol Steroid inhaler Isoproterenol	Asthma exacerbation
Asthma 4	12.5	Male	Asthma	None	Theophylline Steroid inhaler	Viral encephalitis Bronchopneumonia
Asthma 5	1.6	Female	Asthma/ Recurrent pneumonia	None	Quadrinal Antibiotics	Asthma exacerbation
Asthma 6	1.7	Female	Asthma	None	Aminophylline Antihistamine Decongestent	Sepsis Meningitis
Asthma 7	1.8	Female	Asthma	None	Albuterol	Asthma exacerbation
Control 1	8.2	Female	None	Brain tumor	Chemotherapy Radiation Dexamethasone Phenobarbital Propranolol	Brain tumor
Control 2	9.0	Male	None	Brain tumor	Chemotherapy Radiation	Aspiration pneumonia
Control 3	13.6	Male	None	Brain tumor	None	Intracranial hemorrhage
Control 4	13.0	Female	None	None	None	Intracranial hemorrhage and herniation from brain vascular malformation
Control 5	1.3	Male	None	Brain tumor	Chemotherapy Radiation	Metastatic tumor Bronchopneumonia
Control 6	1.7	Female	None	Premature; congenital heart disease (VSD)	Digoxin Chlorothiazide	Sepsis Bronchopneumonia
Control 7	2.0	Female	None	None	None	Meningitis

Table S3. qPCR primers

Actb(β-actin)	5′-CGGCCAGGTCATCACTATTGGCAAC-3′ 5′-GCCACAGGATTCCATACCCAAGAAG-3′
Ascl1	5′-TCTGGCAAGATGGAGAGTGGAGC-3′ 5′-AAAGAAGCAGGCTGCGGGAG-3′
Chga	5′-TTCCCACTTCCATGCAGGCTAC-3′ 5′-GCCTCTGTCTTTCCATCTCCATCC-3′
Calca	5′-CCTTTCCTGGTTGTCAGCATCTTG-3′ 5′-CTGGGCTGCTTTCCAAGATTGAC-3′
Vip	5′-GGCTTTGCAATCCCCAAAGG-3′ 5′-ACACATCCATAGCACACGCA-3′
Npy	5′-TGGCCAGATACTACTCCGCT-3′ 5′-TTGTTCTGGGGGCGTTTTCT-3′
Il5	5′-CCTCTTCGTTGCATCAGGGT-3′ 5′-GATCCTCCTGCGTCCATCTG-3′
Il13	5′-AAAGCAACTGTTTCGCCACG-3′ 5′-CCTCTCCCCAGCAAAGTCTG-3′
Il33	5′-AAGGCGGAATCTGCGTCATT-3′ 5′-TGGTCACACGTGGTTTTGAA-3′
Il25	5′-GCTCCTTTCCCCTGAATCCC-3′ 5′-CAATTACACCTGGCTGCACG-3′
Tslp	5′-AGGGGCTAAGTTCGAGCAAA-3′ 5′-TTTTGTCGGGGAGTGAAGGG-3′
Muc5ac	5′-TGACTCAATCTGCGTGCCTT-3′ 5′-AGGCCTTCTTTTGGCAGGTT-3′
Spdef	5′-GACTGTGGAATTCCTGGGGG-3′ 5′-ATTGTGGCAGGAGCAGAGAC-3′
Foxa3	5′-CTTGGTGGAGGTTGGGTGAG-3′ 5′-ACAGGCAGTATTCCCAAGCC-3′
Il1rl1	5′-TGAGCTGAGGGTGATGAGGA-3′ 5′-GCACGTTCTGGGACATGAGA-3′
Il1rap	5′-FAGAAAGTGCGGCGGAAAGTA-3′ 5′-GACCAGATGGATGCAGGGTG-3′
Calcrl	5′-ACTGTGGTGTCATTCTCAGCC-3′ 5′- ATTGGCACTTCAGCTTTAGAGA-3′
Ramp1	5′- CACTGAGAAATCCGGCCCAT-3′ 5′- CAGTCACACCACAGCGTCTC-3′
Gabrr1	5′- GAGCCCCTGACTCTGTTCAC-3′ 5′- CCTGTGGGCTCAATGCAAAC-3′